NeuroImage 237 (2021) 118188

Contents lists available at ScienceDirect

NeuroImage

journal homepage: www.elsevier.com/locate/neuroimage

Sensory, somatomotor and internal mentation networks emerge dynamically in the resting brain with internal mentation predominating in older age

Lu Zhang[a,b,c,#], Jiajia Zhao[a,#], Qunjie Zhou[a], Zhaowen Liu[d,e], Yi Zhang[a], Wei Cheng[a], Weikang Gong[f], Xiaoping Hu[g], Wenlian Lu[a,b,h], Edward T. Bullmore[i,j], Chun-Yi Zac Lo[a,*], Jianfeng Feng[a,b,k,l,*]

[a] Institute of Science and Technology for Brain-Inspired Intelligence, Fudan University, Shanghai 200433, China
[b] Shanghai Center for Mathematical Sciences, Fudan University, Shanghai, China
[c] Coulter Department of Biomedical Engineering, Georgia Institute of Technology and Emory University, Atlanta, GA, United States
[d] Psychiatric and Neurodevelopmental Genetics Unit, Center for Genomic Medicine, Massachusetts General Hospital, Boston, MA 02114, United States
[e] Department of Psychiatry, Massachusetts General Hospital, Harvard Medical School, Boston, MA 02114, United States
[f] Wellcome Centre for Integrative Neuroimaging (WIN FMRIB), University of Oxford, Oxford OX3 9DU, United Kingdom
[g] Department of Bioengineering, University of California, Riverside, CA, United States
[h] School of Mathematical Sciences, Fudan University, Shanghai, China
[i] Department of Psychiatry, University of Cambridge, Cambridge CB2 0SZ, United Kingdom
[j] Cambridgeshire and Peterborough NHS Foundation Trust, Huntingdon PE29 3RJ, United Kingdom
[k] Oxford Centre for Computational Neuroscience, Oxford, United Kingdom
[l] Department of Computer Science, University of Warwick, Coventry, United Kingdom

ARTICLE INFO

Keywords:
Resting-state fMRI
Dynamic functional connectivity
Connectivity states
Brain functions

ABSTRACT

Age-related changes in the brain are associated with a decline in functional flexibility. Intrinsic functional flexibility is evident in the brain's dynamic ability to switch between alternative spatiotemporal states during resting state. However, the relationship between brain connectivity states, associated psychological functions during resting state, and the changes in normal aging remain poorly understood. In this study, we analyzed resting-state functional magnetic resonance imaging (rsfMRI) data from the Human Connectome Project (HCP; $N = 812$) and the UK Biobank (UKB; $N = 6{,}716$). Using signed community clustering to identify distinct states of dynamic functional connectivity, and text-mining of a large existing literature for functional annotation of each state, our findings from the HCP dataset indicated that the resting brain spontaneously transitions between three functionally specialized states: sensory, somatomotor, and internal mentation networks. The occurrence, transition-rate, and persistence-time parameters for each state were correlated with behavioural scores using canonical correlation analysis. We estimated the same brain states and parameters in the UKB dataset, subdivided into three distinct age ranges: 50–55, 56–67, and 68–78 years. We found that the internal mentation network was more frequently expressed in people aged 71 and older, whereas people younger than 55 more frequently expressed sensory and somatomotor networks. Furthermore, analysis of the functional entropy — a measure of uncertainty of functional connectivity — also supported this finding across the three age ranges. Our study demonstrates that dynamic functional connectivity analysis can expose the time-varying patterns of transition between functionally specialized brain states, which are strongly tied to increasing age.

1. Introduction

Normal aging is associated with the decline of capacity in brain functional flexibility (Geerligs et al., 2014; Malagurski et al., 2020; Monteiro et al., 2019). Cognition requires the dynamic interplay of a set of brain areas functioning as a network rather than as a specific region (la Iglesia-Vaya, 2013). Consequently, functional connectivity (FC) analysis characterizing statistical dependence of two brain regions (Friston et al., 1993), has emerged as an important approach to study the neural mechanism underlying cognitive function (Sala-Llonch et al., 2015; Tomasi and Volkow, 2012). Numerous resting-state fMRI studies

* Corresponding authors.
E-mail addresses: zaclocy@gmail.com (C.-Y.Z. Lo), jianfeng64@gmail.com (J. Feng).
# These authors contributed equally to this work.

https://doi.org/10.1016/j.neuroimage.2021.118188.
Received 7 November 2020; Received in revised form 15 April 2021; Accepted 17 May 2021
Available online 18 May 2021.

have been performed on advanced aging to explore age-related changes in functional connections (Betzel et al., 2014; Chan et al., 2014; Ferreira et al., 2016; Tomasi and Volkow, 2012; Zonneveld et al., 2019) as well as their relation to cognitive performance (Andrews-Hanna et al., 2007; Fjell et al., 2015; Salami et al., 2014; Staffaroni et al., 2018). Despite these advances, most studies on aging estimate the FC over the whole duration of an fMRI scan, potentially obscuring the informative fluctuations in FCs (Naik et al., 2017).

Fransson's pioneering work revealed that the resting brain switches between the introspective and the extrospective states (Fransson, 2005). Following that, recent studies have focused on assessing and detecting the spatiotemporal organization of FC within the brain (Calhoun et al., 2014; Kopell et al., 2014; Preti et al., 2017), and linking the dynamic changes of brain reconfiguration with human demographic indicators, cognition, and disease (Baker et al., 2014; Calhoun et al., 2014; Karahanoglu and Van De Ville, 2015; Zhang et al., 2016). Dynamic functional connectivity (dFC) of resting state fMRI consists of non-random transitions between states or networks of brain regions that can occur over a short time (Calhoun et al., 2014). With a clustering analysis (e.g., k-means or hierarchical clustering), a set of similar time-varying connectivity patterns can be collated, allowing identification of dFC patterns or states that occur consistently across multiple brain regions. These states can be characterized across time and subjects, representing the typical dFC patterns of individuals and a group of subjects in the resting state (Zhou et al., 2019). The brain networks undergoing transitions between states are hierarchically organized (Vidaurre et al., 2017). The variability of state changes is strongly associated not only with demographic characteristics, such as development or gender, but also measures of consciousness and cognition (Preti et al., 2017). This approach offers insight into how the brain is organized, as well as how the connectivity pattern changes over time, and what the relationships are between dynamic functional connectivity and cognitive or behavioural functions.

Dynamic functional connectivity can reveal the functional flexibility in the brain (Allen et al., 2014; Hutchison et al., 2013; Liu et al., 2020; Zhang et al., 2016). Several studies have demonstrated the dFC states change with aging. For example, the temporal variation or state transitions decrease in advanced aging (Chen et al., 2017; Escrichs et al., 2020; Schaefer et al., 2014). Other studies have reported that the elderly spent more time in a state with weak regional interactions and had a lower probability to access the specific state involving the "rich hub" brain area (Escrichs et al., 2020; Tian et al., 2018). Yet Viviano et al. demonstrated there was no difference in the rate of state transitions across the lifespan (Viviano et al., 2017). Thus, the relationship between brain states with cognitive functions and the corresponding state changes in aging remains largely unknown. Conversely, the functional entropy of the brain, which has been utilized to characterize the degree of underlying randomness of the functional connectivity, is increased with age (Yao et al., 2013). This suggests that the changes of dFC states in aging relate to the changes of the uncertainty of FC, represented by function entropy.

The objective of this paper is twofold: to determine the dynamical states that correspond with cognitive functions and to characterize the dynamical state changes in aging. We have analyzed resting-state fMRI (rsfMRI) data from 812 healthy adults, provided by the Human Connectome Project (HCP), to estimate the dynamic whole brain functional connectivity (dFC) states. This was based on a two-step protocol we recently developed for large rsfMRI data sets (Zhou et al., 2019). The dFC was classified into major states, based on a community clustering method from the similarity of dFC across subjects and time. From this we extracted the functional terms with biological significance in the Neurosynth database, using text-mining techniques, and assigned those functional terms to the featured connectivity matrix of each extracted major states by use of an updated Brain Annotation Toolbox (BAT) (Liu et al., 2019). We further estimated the states of aging people from the UK Biobank (UKB) dataset. The dynamic parameters such as occurrence and transition of corresponding states were computed to explore age-related changes of different states; and the functional entropy was also used to estimate the uncertainty of the functional connectivity in aging (Yao et al., 2013).

2. Methods

2.1. Participants and data preprocessing

Two datasets from the HCP and the UKB were used. The brain states and associated cognitive functions during rest were estimated from the HCP; the age-related changes of states with aging were tested from UKB data. The demographic characteristics of participants were described below and summarized in Table 1. See *Supplementary Materials* for detailed imaging preprocessing procedures.

2.1.1. HCP data

The first dataset for this study was collected from the HCP WU-Minn Consortium. The sample included 812 subjects (ages 22–35 years old, of which 450 were female) who were scanned on a 3T Siemens Connectom scanner. For each subject, a three-dimensional T1 structural image was acquired at 0.7 mm isotropic resolution with 3D MPRAGE acquisition. Four rsfMRI runs were acquired in separate sessions on two different days, each running for approximately 15 min, with $2 \times 2 \times 2$ mm^3 spatial resolution, TR = 0.72 s, 1200 time points, and a multiband acceleration factor of 8. Subjects were required to keep their eyes open whilst fixating in a relaxed manner on a projected bright crosshair on a dark background. The WU-Minn HCP Consortium obtained full informed consent from all participants, and research procedures and ethical guidelines were followed in accordance with the Institutional Review Boards (IRB) of Washington University in St. Louis, MO, USA (IRB #20,120,436). For more details, see the HCP website at https://www.humanconnectome.org/. Preprocessing of rsfMRI data, used the HCP Functional Pipeline v2.0 (Glasser et al., 2013), including gradient distortion correction, head motion correction, image distortion correction, and spatial transformation to the Montreal Neurological Institute (MNI) space, with one step spline resampling from the original functional images. The linear trend and quadratic term were removed from these functional images, and several nuisance signals were regressed from the time course of each voxel using multiple linear regression, including cerebrospinal fluid, white matter, and 24 head motion parameters (Friston et al., 1996). Finally, temporal band-pass filtering (0.01–0.1 Hz) was performed to reduce the influence of low-frequency drift and the high-frequency physiological noise.

2.1.2. UKB data

The second dataset included 6716 subjects (ages 50–78 years, mean age ± SD 62.62 ± 6.89 years old, of which 3909 were female). FMRI data of UKB parallel the HCP dataset and were collected on a 3T Siemens Skyra scanner. For each subject, a three-dimensional T1 structural image was acquired at 1 mm isotropic resolution with 3D MPRAGE acquisition. RsfMRI data were acquired with $2.4 \times 2.4 \times 2.4$ mm^3 spatial resolution, TR = 0.735 s, 490 timepoints in 6 mins, multiband acceleration factor of 8, with eyes open and fixated on a crosshair. The UK Biobank obtained full consent from the participants, with IRB approval of the North West Multicenter Research Ethics Committee. For more details, see the UKB website at https://www.ukbiobank.ac.uk/ . The preprocessing procedures for the UKB fMRI dataset involved slice-timing correction, motion correction, spatial smoothing, nuisance signals removal, bandpass filtering, and spatial normalization (see *Supplementary Materials* for more details). The volume-to-volume head motion, a.k.a. framewise displacement (FD), was used to estimate the head movement and to provide a quality control criterion to exclude fMRI datasets with mean FD > 0.3 mm. For age comparisons, the UKB data were divided into nine age groups from 50 to 73 years, with an interval of 3 years,

Table 1
The demographic characteristics of participants.

	Basic information								
	Age (year)	Gender(Male / Female)	Handedness (right/left/both)	Race(White / Others)	Education (years)	BMI	BPDiastolic	BPSystolic	Head Motion
HCP	28.76±3.71	362/450	722/61/29	603/209	14.93±1.79	26.37±5.09	76.67±10.50	123.69±13.92	0.35±0.14
UKB	62.62±6.89	2807/3909	5995/615/104						

Note: HCP, Human Connectome Project. UKB, UK Biobank. The original score of handedness in HCP is 65.87±44.15, the handedness of right, left, and both were thresholded by 25, −25, and between.

and a group range from 74 to 78 years for an appropriate number of subjects in other age groups.

2.2. Dynamic whole-brain functional connectivity categorization

One hundred and twenty regions from the automated anatomical labeling 2 template (AAL2, (Rolls et al., 2015)) were used to parcellate the brain, before estimating the regional mean rsfMRI signal of all voxels within each region (Supplementary Table 1). We also assigned the AAL2 regions to Yeo's seven functional modules according to the most overlapping ratio (the percentage of voxels of a specific region with each module) (Yeo et al., 2011). The cerebellum and subcortical regions were added as two additional modules. The FC matrix comprises all possible pair-wise Z-transformed Pearson's correlations between regional rsfMRI signals. Dynamic functional connectivity (dFC) was represented by a time series of whole brain FC matrices, each matrix capturing functional connectivity over a period of time, or window-length, less than the total length of the rsfMRI signal. We used a fixed window length of 20 sampling points (14.4 s), non-overlapping windows to estimate dFC. A two-step community clustering of the dFC was further applied, to detect distinct brain network states in the HCP data sets (Zhou et al., 2019), see *Supplementary Materials* for more details. Noted that using other window-lengths (10, 30, 40 and 50) had a minor effect on the clustering results (Zhou et al., 2019). In this study, the HCP data was used to detect the dFC states, as the dataset has high spatial and temporal resolution and each subject was repeatedly measured four times. After state detection, the "average" functional connectivity of each state was defined as the average of all dFC in the corresponding community. The "feature score", the correlation coefficient between two FC matrices, was used to classify the dFC of UKB dataset into three states (Zhou et al., 2019). The state of each dFC in the UKB data was determined by retrieving the highest feature score for the corresponding state, without applying community detection on the UKB data again. The similarity of classified dFCs between HCP and UKB for each state was estimated.

2.3. Functional annotation for the feature circuits

The Brain Annotation Toolbox (Liu et al., 2019) (BAT; available online at http://www.dcs.warwick.ac.uk/~feng/BAT), which is based on the Neurosynth database (http://neurosynth.org), was modified for this study in order to explore the underlying functional implications of the three states. A total of 217 functional terms, bearing clear biological significance, were collected from 11,000 journal articles using text-mining techniques. For a given function term such as "primary visual", activation times of a given voxel across different studies were calculated. Therefore, each voxel was associated with a number of terms or tasks that can help us to interpret the function in a specific region, as well as a specific FC or FC networks (see *Supplementary Materials* for more details). For each state, the featured FC was tested to the relevant functional terms by the normalized activation ratio of each functional term. The distribution of the activation ratio under random conditions was obtained by randomly permuting the brain regions ~10,000 times so that the significance ($P < 0.05$, Bonferroni corrected) of each functional term could be identified. See *Supplementary Materials* for more details.

2.4. Correlational analysis between the dynamic parameters and the behavioural tests

To assess the relationships between connectivity dynamics and behavior, a canonical correlation analysis (CCA) was used to determine the significance of association between the dynamic parameters (occurrence, transition rate, and mean persistence time) and specific behavioural traits. In total, 266 behavioural traits were used, excluding poor quality and missing measures (Smith et al., 2015) (see Supplementary Table 2 for the measures used). Via a rank-based inverse Gaussian transformation, all measures were converted into normalized Z scores and reduced to 100 dimensions using principal component analysis (Abdi and Williams, 2010). Linear regression was used to determine both the dynamic parameters and the behavioural traits, with the following covariates: sex, age, handedness, body weight, height, education years, body mass index (BMI), systolic blood pressure, diastolic blood pressure, and mean FD. The CCA was performed for the dynamic parameters and 100 principal components of the behavioural traits. This included 10 behavioural domains (cognition, alertness, emotion, task performance, health and family history, personality, psychiatric and life function, sensory and motor, and substance use). Furthermore, the correlations between canonical covariates of behavioural traits and dynamic parameters were estimated.

2.5. Entropy

The entropy defined by Shannon (Shannon, 1951) was used to measure the uncertainty of the functional connectivity in aging from the UKB dataset. First, we estimated the static functional connectivity by calculating the Pearson correlation between the whole time series of 120 regions in AAL2. Second, we discretized all functional connectivity from −1 to 1 into 20 intervals with equal width and counted the frequency (p_i) of each class to estimate its probability distribution (Yao et al., 2013). The regional-level entropy was calculated as Shannon entropy ($-\sum_{1\le i\le 20} p_i \log(p_i)$) according to the discrete distribution of functional connectivity linking to a specific region. The whole brain functional entropy was the average entropy of individual brain regions estimated for each subject.

2.6. Statistical analysis

Both the functional annotation for the states and the relationship between the dynamic parameters and behavioural traits were analyzed by permutation tests (10,000 times, with Bonferroni correction for multiple comparisons). To test for dynamic changes in aging, the trends of dynamic parameters were detected by the Jonckheere-Terpstra test (Bewick et al., 2004), and post-hoc between group comparisons were performed by two sample t-test with FDR correction, after regressing out the mean FD by a general linear model. The significance level for all statistical tests was set at $P < 0.05$ after multiple comparisons correction if needed. The similarity between FC entropy of different age groups was defined by the P value of two sample t tests. The age categorizations were detected using the Louvain algorithm according to the similarity matrix (Le Martelot and Hankin, 2013).

2.7. Ethics statement

The WU-Minn HCP Consortium obtained full informed consent from all participants, and research procedures and ethical guidelines were followed in accordance with the Institutional Review Boards (IRB) of Washington University in St. Louis, MO, USA (IRB #20120436). For more details, see the HCP website at https://www.humanconnectome.org/. The UK Biobank obtained full consent from the participants, with IRB approval of the North West Multicenter Research Ethics Committee. For more details, see the UKB website at https://www.ukbiobank.ac.uk/.

3. Results

3.1. The dynamic FC and three functional states

To characterize the dynamics of functional connectivity, all BOLD signals were segmented into non-overlapping sliding windows and the time-varying FC matrices were estimated from HCP data: in total 240 FC matrices, each estimated in 60 time windows in each of 4 scanning sessions (Fig. 1A). Three community structures were detected in our previous work through a second-level community clustering algorithm (Fig. 1B) (Zhou et al., 2019). The functional connectivity of three distinct states was estimated by the average of all dFC in the corresponding community (Fig. 1C), denoted as featured dFC matrix. Thus, each window-based dFC from one given subject could be assigned to one of the three states (Fig. 2A, B). The three states tended to alternate with a probability of 0.58, 0.56 and 0.55 respectively, rather than stay in the same state. For UKB data, each dFC was assigned to one of the three states according to the highest feature score, defined as the correlation coefficients with featured dFC matrix from HCP data. The state sequences were then used for the consequent analyses on aging. The Pearson correlation coefficient between the three feature networks in HCP and UKB was higher than 0.8, showing the consistency between two datasets.

3.2. Activated FCs of the three dFC states and their functions revealed by literature mining

In order to investigate the functional implication of the three states detected, firstly we assigned the AAL2 regions to Yeo's seven functional modules (Yeo et al., 2011) (see Method), together with cerebellum and subcortical modules, to reveal the mostly activated functional modules of the three states. Further, we addressed the function of the detected dFC states based on more comprehensive knowledge by text mining from 11,000 published journal articles. The featured connectivity matrix of each state was estimated by BAT for the activations and significance of functional terms within each state (Fig. 1D). The significant related functional terms were sorted by a normalized activation ratio, to present the correlation between the FC patterns and functions (permutation test, $P < 0.05$, Bonferroni corrected). For state 1, the strongest FCs were within and between visual, somatomotor, attention and cerebellum modules (Fig. 2A, left), and 40.5% and 32.5% of the top 200 FCs were related to visual and somatomotor modules, respectively (Table 2). Comparable with that, the top 10 most significantly related functional terms were related to vision processing, visual attention, and sensorimotor functions (Fig. 2C). State 2 shared similar FCs with state 1 except the weaker activated visual module (Fig. 2A, middle; Table 2), more dominant activation of somatomotor modules (47.0% of the top 200 FCs). The FC links within and between limbic, default mode and frontoparietal modules were more involved than those in state 1 (Fig. 2A). The most related function terms of state 2 were auditory and languages functions (Fig. 2C), comparable with the highly activated STG, HES for sound processing, and IFGoperc, IFGtriang (Broca's area), ANG, SMG (part of Wernicke's area), STG, MTG for languages (Fig. 2A, middle). Besides, multisensory and touch terms were also involved in state 2 (Fig. 2C), associated highly activated regions for sensorimotor functions including PreCG, PoCG, SMA and ROL (Fig. 2A, middle). State 3 was found to be highly involved with default network (45.0% of the top 200 FCs), limbic and cerebellum modules (Fig. 2A, right; Table 2), which was related to self-referential processes and theory of mind (Fig. 2C). Finally, according to neural substrates and their functions revealed above, we defined these three states as "sensory network", "somatomotor network", and "internal mentation network" for state 1, 2, and 3, respectively. Note that the three labels did not fully characterize the three states in the domain of functional terms. Some of the most relevant functions were found to be commonly involved among connectivity states. Multisensory and touch terms were both associated with sensory and somatomotor networks, and the language-related functions were involved in somatomotor and internal mentation networks. The results for second-level network functions of the substates were illustrated in Supplementary Fig. 2.

3.3. Association of dFC state features with human behaviour

As dFC represented different brain functional networks, it is important to know whether the persistence or switching between networks is associated with behavior. The occurrence, transition rate, and mean persistence time among states, were calculated as dynamic features, and we further investigated their correlation with behavior. With canonical correlation analysis (CCA), we found a significant correlation between behavior and the dynamic parameters ($r = 0.48$, $P = 0.0092$, permutation test). The dominating behavioural scores which explained variance > 3% in the principal canonical covariate of behavioural traits (CCA mode) are illustrated in Fig. 2D. behavior including processing speed and accuracy in cognition tasks were positively correlated with the CCA mode. These behaviours were positively associated with cognitive ability and referred to as positive behavioural scores (the higher, the better). In contrast, negative behavior, including reaction time on cognition tasks, the Pittsburgh Sleep Quality Index (PSQI) score, Diagnostic and Statistical Manual of Mental Disorders and Adult Self-Report scores, were negatively correlated with the CCA mode (Fig. 2D). Occurrence and mean persistence times of sensory network (state 1), as well as the transition rates from internal mentation to sensory networks (state 3 to 1) were highly associated with the principal behavioural CCA mode as well as positive behavioural scores (Fig. 2E). Whereas occurrence and persistence time of the somatomotor network (state 2), as well as the transition rate from internal mentation to somatomotor networks (state 3 to state 2), were negatively correlated with the CCA mode, which indicates their association with negative behavioural scores (Fig. 2E). Internal mentation network (state 3) was less strongly associated with behavior (explained variance < 3%) compared to the other two states.

3.4. Functional connectivity states in aging

The states of each dFC in aging from UKB data were determined by their correlation coefficients with the three featured dFC matrices from HCP data, denoted as a feature score. Then each individual dFC was assigned to the dFC state with the highest feature score. To ensure the association of dynamic features of the dFC, the related brain functions of the featured connectivity matrix of each state from the UKB data were examined by BAT and the results were similar to HCP, i.e., the sensory, somatomotor, and internal mentation networks (Supplementary Fig. 1). The mean frequencies of occurrence of each of the 3 states defined in the HCP dataset were 26%, 20%, and 54% for sensory, somatomotor, and internal mentation states, respectively, in the UKB dataset. The occurrence of all three states was changed with aging (Fig. 3A, Supplementary Fig. 3), showing a significantly increasing trend, from 50 to 78 years, in the internal mentation network ($Z = 7.60$, $P = 1.43 \times 10^{-14}$, Jonckheere-Terpstra test) and a decreasing trend in the sensory ($Z = -5.64$, $P = 8.44 \times 10^{-9}$, Jonckheere-Terpstra test) and so-

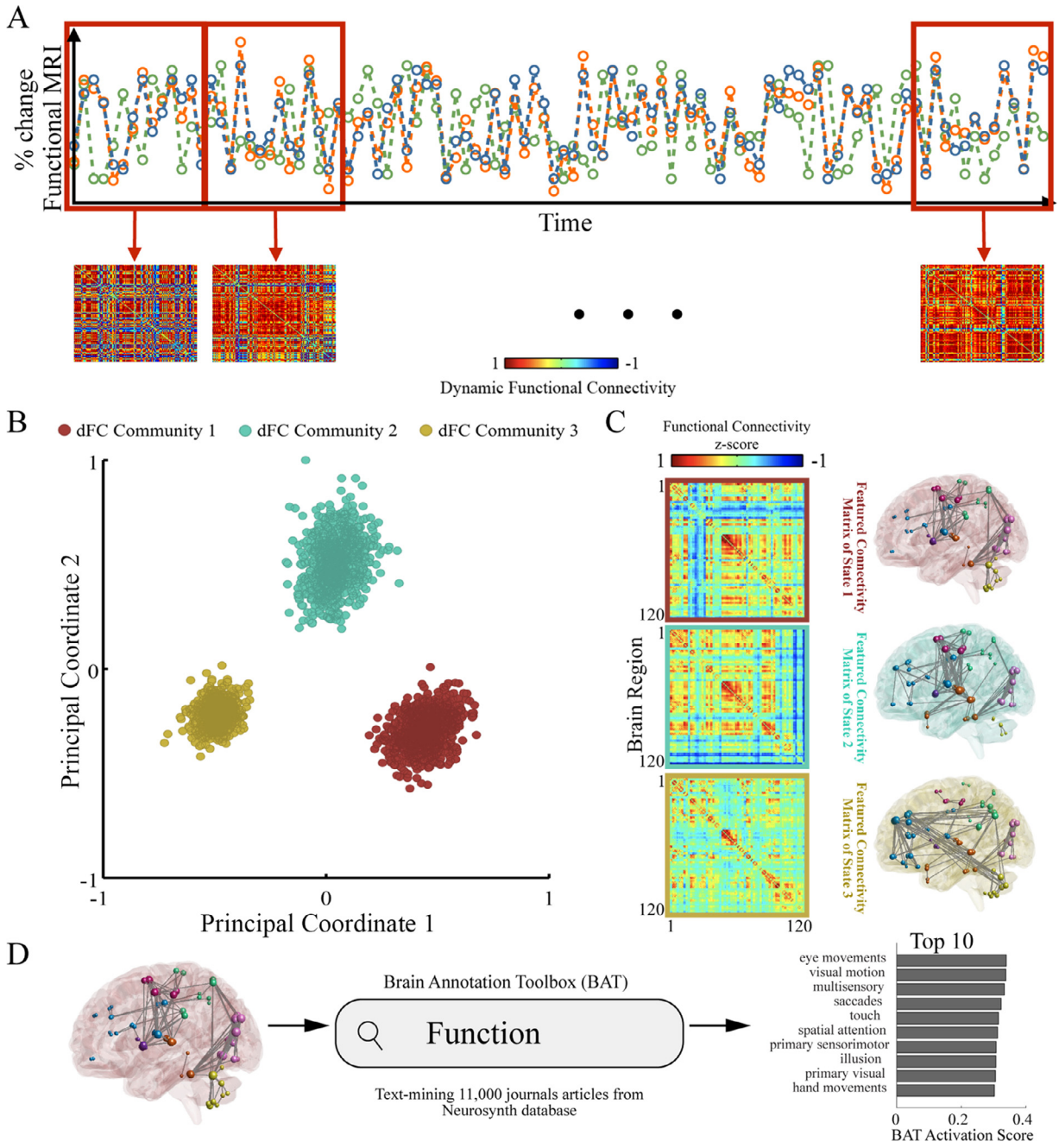

Fig. 1. State detection and the feature network of dynamical whole brain functional connectivity. A. The whole brain dynamic functional connectivity was estimated with non-overlapping sliding window (length of 20 time points). B. The scatter plot of clustered dFCs in principal coordinate analysis. Distance between dFC points is defined by 1-correlation$_{dFC\text{-}dFC}{}^2$, where principal coordinate analysis projects those dFC points into 2D spaces while preserved the original distance as much as possible. All dFCs were detected across subjects and time into three states. Each dot represented the averaged dFC of one state for a given subject. C. The corresponding features (averaged dFCs in the same states) for three states (left) and top 200 FCs (right). The automated anatomical labeling 2 atlas was used and the abbreviations are listed in Supplementary Table 1. D. Example illustration of searching function term for the featured dFC networks in C (state 1) using Brain Annotation Toolbox (BAT). Top 10 significant enriched functional terms were shown, with activation ratio sorted from top to down. See method and *Supplementary Materials* for more details.

matomotor networks ($Z = -4.02$, $P = 2.93 \times 10^{-5}$, Jonckheere-Terpstra test). The occurrence of the sensory network was found to be significantly decreased in people after 71 (Fig. 3A, B left; two sample t-test, $q < 0.05$ FDR correction for 108 comparisons). The occurrence of the somatomotor network was found to be significantly decreased in people after 56, compared to people before 53 (Fig. 3A, B middle; two sample t-test, $q < 0.05$ FDR correction for 108 comparisons). The occurrence of the internal mentation network was found to be lowest in people younger than 55, intermediate between ages 56 to 67, and highest above 68 (Fig. 3A, B right; two sample t-test, $q < 0.05$ FDR correction for 108 comparisons). With age, the transition rate from the internal mentation network to other states decreased, and that from others increased, i.e., more states were found to transition to the internal mentation network with age (Fig. 3A). There was no significant difference in mean persistence time of sensory and somatomotor networks among all age groups, but a significant increase in mean persistence time of the internal mentation network was found between people before 67 and people after 71.

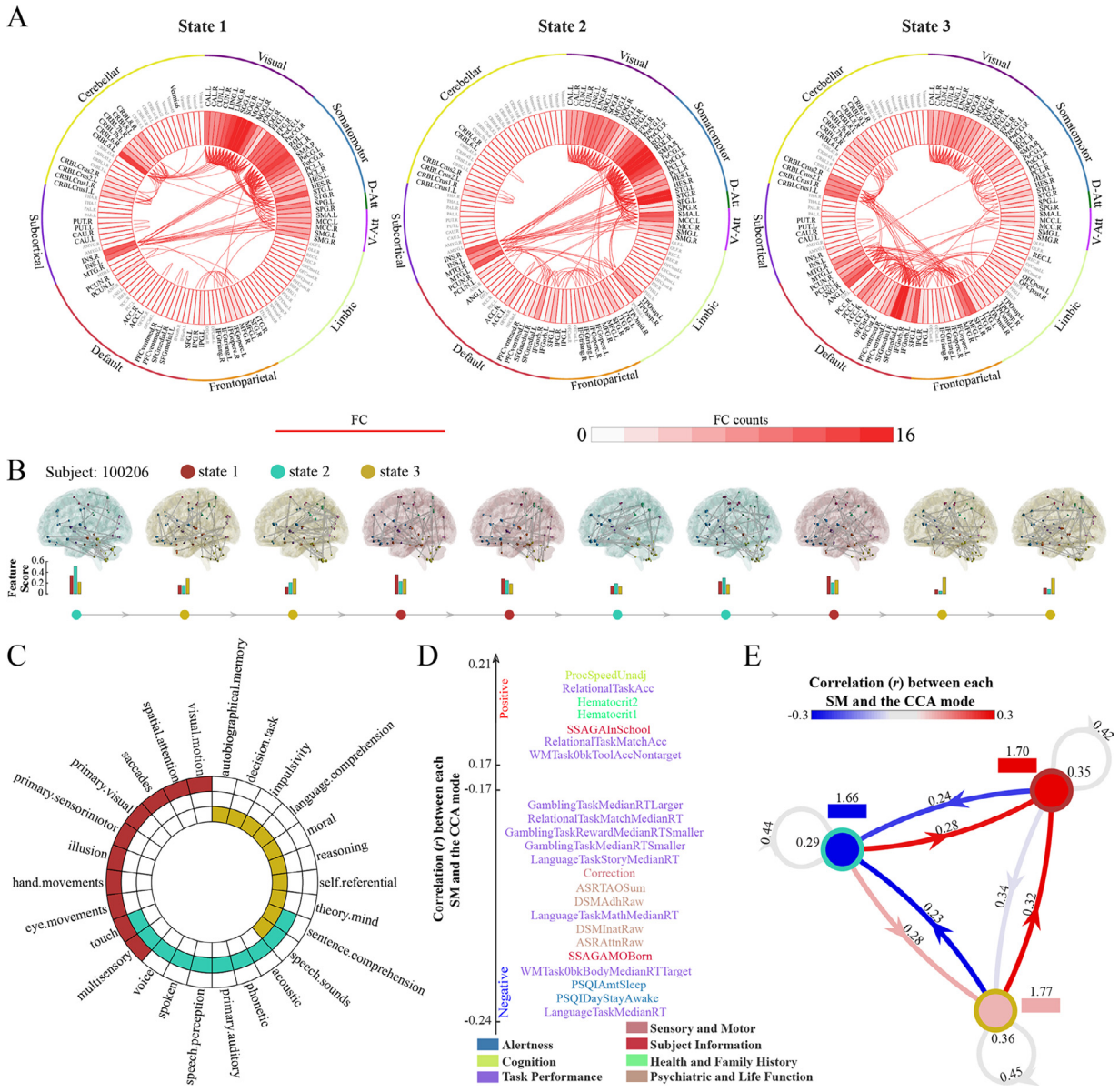

Fig. 2. The function and association with the behavior of whole brain functional connectivity states. A. The corresponding features (averaged dFCs in the same states) for three states and top 200 FCs. The AAL2 atlas was used and the abbreviations are listed in Supplementary Table 1. B. Ten consecutive sliding-window-based dFC calculated from one HCP subject (ID:100,206), in which the top 100 FCs were shown on the second row. The feature scores, correlation coefficients between each window-based FC matrix, and "average" functional connectivity of three states were shown with histogram. Each dFC was assigned into three of the dFC states shown with the colored dot (red: state 1; green: state 2; yellow: state 3). C. Top 10 significant enriched functional terms were extracted by Brain Annotation Toolbox (BAT) from network composed by the whole brain FC in each dFC state (color-filled, from outer to inner). For dFC state 1, the most significantly enriched functional terms (noted in red) were related to vision and sensation; state 2 was related to the acoustic and languages terms (noted in green); state 3 was significantly related to self-referential and theory of mind (noted in yellow). D. The set of behavioural trials most strongly associated with the principal behavioural CCA mode of population variability (variance explained > 3%). Colors represent different domains and vertical position is according to the correlation between CCA mode. The color indicates the categories of behaviour traits. E. Correlation between dynamic parameters and the principal behavioural CCA mode was shown as a heat map. The red color indicates a positive correlation, and the blue color indicates a negative correlation. Occ: occurrence is shown by the circle; MPT: mean persistence time shown by square; TR: transition rate shown by the directed arc. Occ, MPT and TR values were shown along with the circles, squares and arrows, respectively. Noted that self-transition rate of the three states was not involved in the correlation with the CCA model, as they could be calculated from other inter-state transitions.

3.5. The relationship between the internal mentation state and functional entropy

We further estimated the functional entropy, which measures the dispersion and randomness of functional connectivity within the brain, for each subject in different age groups (Yao et al., 2013). Low entropy shows that the functional connectivity has a high level of predictability with a low level of randomness, and vice versa for high entropy. Pairwise comparisons of all age groups revealed three age categorizations based on entropy: 50–55 years, 56–67 years and 68–78 years (Fig. 3C), which was similar to the dynamic features of state 3, the internal mentation network (Fig. 3B right). A remarkable correlation was found between entropy and the occurrence of the internal mentation network with age ($r = 0.80$, $P = 2.23 \times 10^{-7}$, Fig. 3D), indicating the occurrence or transition to the internal mentation state is consistent with a high level of randomness of FC during the aging process.

Table 2
The percentage of top 200 FCs associated with nine functional modules of three states.

Percentage (%)	State 1 FCs			State 2 FCs			State 3 FCs		
Function Modules	All	Within module	Between modules	All	Within module	Between modules	All	Within module	Between modules
Visual	**40.5%**	32.5%	8.0%	27.5%	25.0%	2.5%	20.5%	20.5%	0.0%
Somatomotor	32.5%	22.0%	10.5%	**47.0%**	28.5%	18.5%	10.5%	8.5%	2.0%
D-Att	6.5%	0.5%	6.0%	2.0%	0.5%	1.5%	1.0%	0.5%	0.5%
V-Att	12.5%	2.0%	10.5%	14.0%	1.5%	12.5%	4.0%	1.0%	3.0%
Limbic	0.5%	0.0%	0.5%	7.0%	1.5%	5.5%	8.5%	2.0%	6.5%
Frontoparietal	5.0%	2.5%	2.5%	6.0%	2.5%	3.5%	15.5%	5.0%	10.5%
Default	3.5%	2.0%	1.5%	16.0%	7.0%	9.0%	**45.0%**	26.5%	18.5%
Subcortical	11.0%	1.5%	9.5%	9.5%	0.5%	9.0%	2.0%	1.5%	0.5%
Cerebellar	15.0%	10.0%	5.0%	2.0%	2.0%	0.0%	17.0%	10.5%	6.5%

All refer to FC connected at least one of the regions in a specific module. Noted that the highest active modules are visual, somatomotor, and default networks for the three states, highlighted in bold font. Importantly, results are comparable when using top 100 FCs (visual 50.0%, somatomotor 45.0%, and default network 39.0%, for the three states) and 300 FCs (visual 38.3%, somatomotor 45.7%, and default network 49.0%, for the three states).

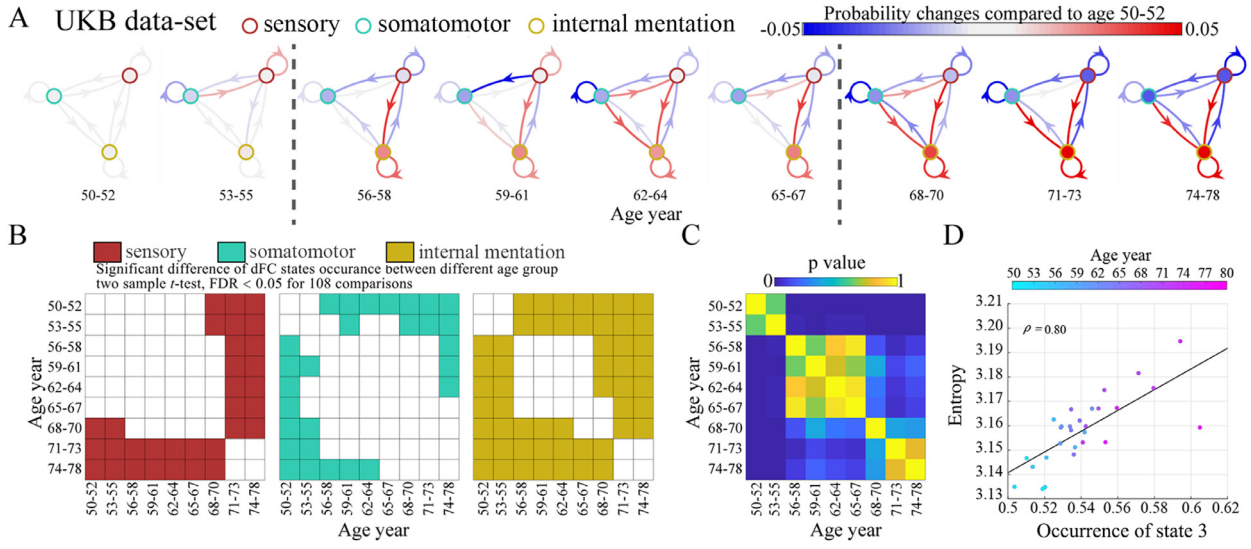

Fig. 3. The dynamic parameters in aging. A. The occurrence (nodes) and transitions (directional arcs) of three states change with age, referring to the first age group (50–52). The heat map illustrates the mean value in each group subtracted with the first group (50–52). The transition rates from the state 1/2 to the state 3 were increased with age. Both the occurrences of state 1 and 2 (sensory and somatomotor) had significant decreased trend, and the occurrence of state 3 (internal mentation) had significant increased trend (sensory: $Z = -5.64$, $P = 8.44 \times 10^{-9}$, somatomotor: $Z = -4.02$, $P = 2.93 \times 10^{-5}$, self: $Z = 7.60$, $P = 1.43 \times 10^{-14}$, Jonckheere-Terpstra test). The vertical dashed lines indicate a similar pattern of functional dynamics in the three age ranges, i.e., 50–55, 56–67, and 68–78, see B for references. B. The group comparison between ages. The colored elements indicate the significant differences by the post-hoc comparison among the age groups and states (two sample t-test, $q < 0.05$ FDR correction). Note that there were 636, 668, 767, 820, 916, 1041, 977, 563 and 328 subjects in each group from the youngest to the oldest, respectively. C. The P value matrix of the comparison of functional entropy among the age groups (two sample t-test). Significant differences were also found around 55 years and 68–70 years. D. The correlation between functional entropy and the occurrence of state 3. Each dot represents a year with its color indicating the age ($r = 0.80$, $P = 2.23 \times 10^{-7}$).

4. Discussion

Combining data-driven methods for dynamic functional connectivity analysis of rsfMRI, and comprehensive literature searching, our study revealed that the brain connectivity in the resting state consists of three major brain states: “sensory network”, “somatomotor network”, and “internal mentation network”. The dynamic parameters of the connectivity states (i.e., occurrence, transition rate, and mean persistence time) were found to be mainly associated with behavioural scores relating to task performance, alertness, and cognition, as well as psychiatric and life functions. By estimating the connectivity states in the UKB dataset, we found a significantly higher transition to “internal mentation network” in aged people, revealing three aging levels in the dynamic whole brain connectome. Importantly, such aging effects were compatible with additional FC entropy analyses. Our findings show, for the first time, that the functional dynamics in resting state expose the full picture of the related brain functions of the whole-brain connectome, and the brain activity reveals the network-level changes associated with aging.

In recent years, understanding the time-varying networks in rsfMRI studies (Calhoun et al., 2014; Cavanna et al., 2018; Pinotsis et al., 2013; Preti et al., 2017) has played an important part in revealing the fundamental mechanisms operating in the brain. However, wide heterogeneity was found across different studies (Damaraju et al., 2014; Faghiri et al., 2018; Kim et al., 2017). Sliding window correlations were mostly used to calculate dynamic functional connectivity in prior studies (Hutchison et al., 2013; Reinen et al., 2018; Thompson, 2018). However, a recent study questioned the validity of dFC detection methods, pointing out the necessity of increased session and subject-averaging measures (Hindriks et al., 2016). To address this concern, we used a community clustering method to detect the connectivity states, which are robust across various window lengths and groups of subjects (Zhou et al., 2019). Thus, our results of connectivity states were derived from a large data set with a high temporal and spatial resolution, with scanning repeated four times for each subject.

The dynamic changes of network patterns are on a continuum, being more integrated (a wider extent of connections between distinct regions)

or segregated (wider extent of connections within tight-knit linking of regions) (Shine et al., 2016). In these three states, the sensory and somatomotor networks (state 1 and 2) tend to be integrated, whereas the internal mentation network (state 3) tends to be segregated. Our results are consistent with the findings from Shine et al. (2016) as states 1 and 2 are related to sensory and attention networks, whereas state 3 is related to default mode network (DMN) (Shine et al., 2016). The dominant functional module of sensory state (state 1) is visual networks, with somatomotor and attentional networks also highly activated. Those networks are largely involved in the tasks requiring interactions with the external environment (Corbetta and Shulman, 2002), thus state 1 is considered as an externally oriented state (Hugdahl et al., 2015; Zabelina and Andrews-Hanna, 2016). While in the somatomotor state (state 2), the somatomotor module is the most activated modules, including the highly activated regions for sensorimotor functions (PreCG, PoCG, SMA, and ROL)(Brown et al., 2005; Koelsch et al., 2006; O'Regan and Noe, 2001), regions relate to acoustic, speech and other languages process (TPOsup, STG, MTG and HES)(Nakamichi et al., 2018; Tomasino et al., 2015), as well as other regions relate to decision-making including PFCventmed, SFGmedial, ACC (Alexander and Brown, 2011; Hampton and O'Doherty J, 2007), the state 2 is considered as an action-oriented state. Noted that, sensory (state 1) and somatomotor (state 2) networks can be generalized as external oriented, as sub-states of the extrinsic networks proposed by Golland et al. (Golland et al., 2008). In this work, we distinguish the two states from the extrinsic networks. The functional network of state 1 (sensory, external oriented) represents the sensory inputs from the external environment, while the functional network of state 2 (somatomotor, action oriented) represents sensory-guided motor actions with feedbacks to the environment (Fuster, 2001, 2004). In contrast, the internal mentation network can be considered as an internally oriented state (Buckner and Carroll, 2007; Zabelina and Andrews-Hanna, 2016), considering the crucial role of DMN in internally-oriented cognition (Andrews-Hanna et al., 2010; Spreng, 2012). Additionally, previous researches suggest the salience network, include insula and anterior cingulate cortex (ACC), is responsible for switching between intrinsic and extrinsic networks (Goulden et al., 2014; Sridharan et al., 2008). The insula and ACC have reciprocal connectivity with one other, which are also reciprocally connected with motor and sensory areas of the brain (Goulden et al., 2014). In line with these results, our study showed that the insula was strongly connected with somatomotor and attention networks in state 1 and 2, while ACC was strongly connected with the DMN in state 3 (Fig. 2A). Another unclear issue regarding dFC states is their psychological or biological significance. Yet, using BAT, we were able to link the most relevant cognitive functions and the connectivity patterns in each state. Our finding of the internal mentation network (state 3) is consistent with prior literature, as resting brain activity is associated with high-order cognitive processes, such as moral reasoning or self-consciousness (Buckner et al., 2008; Morcom and Fletcher, 2007).

Summarizing the studies on the major psychopathologies, Menon proposed a triple network model which includes the central executive network (CEN), salience network (SN) and DMN (Menon, 2011); and Karahanoglu summarized 13 dynamic brain states into attention, sensory and a default model (Karahanoglu and Van De Ville, 2015). The three states we found were compatible with these findings, linking brain activity and function. However, the cerebellum was not included in the previous studies, although we found it participates heavily in sensory and internal mentation networks (states 1 and 3). Growing evidence supports cerebellar participation in general cognition (Ramnani et al., 2006), where the cerebellum plays a role as an adaptive filter, decorrelating its input signals during both motor and non-motor cognition with error messages (Fujita, 1982; Porrill et al., 2013; Wolpert et al., 1998). In this study, we investigated the dynamic fluctuations in whole brain functional connectivity in humans. More importantly, previous studies interpreted the identified brain networks with a limited or hypothetically selected literature. Instead, the labeling of the sensory, somatomotor and internal mentation networks in this study was based on comprehensive knowledge summarized from thousands of independent studies in the literature, using BAT. We characterized the full picture of the spatiotemporal organization of the human brain, and its projection in cognitive and functional domains.

By applying these connectivity states to an independent dataset (UKB), the age effect on the occurrence of the three states was demonstrated in people older than 50 years. We found that the occurrences of state 3, the internal mentation network, were increased with age. A remarkable pattern was found that the occurrence or transition of state 3 was distinct between three groups: 50–55, 56–67, and 68–78 years. Meanwhile, the decreasing occurrence of sensory networks was found after 68–70 years. These results suggest that people older than 67 are more frequently transitioning to the internal mentation network, and less frequently to the sensory and somatomotor networks during resting state. This finding is consistent with previous reports that the elderly were likely to spend more time in a connectivity state with lesser connectivity between DMN and somatosensory/visual module, and greater connectivity between DMN and cerebellum/subcortical module (Viviano et al., 2017). On the other hand, it has been found that regions with large entropy tend to maintain relatively high functional connectivity with many other regions in different time windows and therefore demonstrate low temporal variability (Zhang et al., 2016). We found a similar cutoff age (between 55 and 68 years) to that revealed by dFC dynamic parameter variation by analysis of the age-related changes in entropy. We have demonstrated that the connectivity state of brain dynamics changes with aging, affecting sensory, somatomotor, and internal mentation networks. These results generated an intuitive biological conjecture that the degradation of physiological function accompanying aging, such as vision problems and hearing loss, could be related to the dynamic characteristics of brain connectivity. The brain of the elderly tends to stay in the "self-awareness" mode. Thus, our findings may be a potential biomarker of brain connectivity in aging and age-related functions.

There are several potential limitations regarding our methodology. As the head motion is a crucial factor for fMRI, the denoising step in data preprocessing was not sufficient. We also used mean framewise displacement (FD) as a covariate when performing the statistical analysis. On the other hand, the BAT is based on a comprehensive literature search, however, the existing literature might not target all brain functions or related regions equally. This might partially contribute to the following two unsolved issues. First, the characterization of the three networks in the domain of the functional terms is not centralized. For example, the multisensory term is involved in both sensory and somatomotor networks, and language-related functions were involved in somatomotor and internal mentation networks. This is not completely surprising as we expect the function term is not independent with each other, requiring the participation of the overlapped brain networks. Second, the neural substrates of the three networks did not match the functional terms perfectly. In future works, we would further explore the optimized parameterization in using BAT, and additional novel findings could be added to the literature domain to further improve the significance of our methods.

In conclusion, we identified the relevant brain functions of connectivity states to reveal the full picture of the brain activity and the functional implications of dynamic connectivity changes during rest. Age-related changes in the functional dynamics among sensory, somatomotor, and internal mentation networks have a physiological meaning and might serve as a neuroimaging marker of aging. This work can help to understand brain activity and its associated functions, and may further be applied to task-evoked data. We expect that the detection of the connectivity states and their changes with age will open future investigations of age-related brain functions and cognitive functions, and link other brain characteristics such as brain morphometry or neuronal connections.

Declaration of Competing Interest

Nothing to declare.

Acknowledgement

This study was supported by the Shanghai Municipal Science and Technology Major Project (No. 2018SHZDZX01), National Key R&D Program of China (No.2018YFC1312900), the key project of Shanghai Science and Technology (No. 16JC1420402), the National Key Research and Development Program of China (No. 2018YFC0910503), the Young Scientists Fund of the National Natural Science Foundation of China (No. 81801774), Natural Science Foundation of Shanghai (No. 18ZR1403700), Guangdong Key Research and Development Project (No. 2018B030335001), the Shanghai Science and Technology Innovation Plan (Nos. 15JC1400101 and 16JC1420402), the Base for the Introducing Talents of Discipline to Universities (No. B18015), the National Natural Science Foundation of China (Grant Nos. 71661167002 and 91630314), the China Postdoctoral Science Foundation (2016M591590), the 111 Project (No. B18015). JF was a Royal Society Wolfson Research Merit Award holder. ETB was supported by an NIHR Senior Investigator Award. We thank Dr. David Waxman and Dr. Ashley Prichard for helpful suggestions during the manuscript writing.

Credit author statement

Lu Zhang: Conceptualization, Methodology, Software, Investigation, Formal analysis, Validation, Writing- Original Draft, Writing- Reviewing and Editing, Visualization. **Jiajia Zhao**: Investigation, Formal analysis, Validation, Writing- Original Draft. Writing- Reviewing and Editing, Visualization. **Qunjie Zhou**: Software, Investigation, Formal analysis, Data Curation, Validation, Writing- Original Draft, Writing- Reviewing and Editing, Visualization. **Zhaowen Liu**: Software, Investigation, Resources. **Yi Zhang**: Software, Investigation, Formal analysis, Data Curation, Validation. **Wei Cheng**: Software, Investigation, Resources. **Weikang Gong**: Software, Investigation, Resources. **Xiaoping Hu**: Methodology, Writing- Original Draft. **Wenlian Lu**: Methodology, Software. **Edward T. Bullmore**: Writing- Original Draft. **Chun-Yi Zac Lo**: Conceptualization, Methodology, Software, Investigation, Resources, Formal analysis, Data Curation, Validation, Writing- Original Draft, Writing- Reviewing and Editing, Visualization, Supervision. **Jianfeng Feng**: Conceptualization, Methodology, Writing- Original Draft, Supervision.

Data and code availability statements

The first data used in current study is obtained from HCP WU-Minn Consortium, the full dataset and documentation are openly available at https://www.humanconnectome.org/. The second data is obtained from UK biobank database, which can be requested to download from UKB website at https://www.ukbiobank.ac.uk/. All code for data cleaning and analysis in current study is provided as part of the replication package. It is available at https://www.dropbox.com/sh/74oc0l55qayc42x/AABsxs5i2onrpDXVqutwlsxJa?dl=0.

Supplementary materials

Supplementary material associated with this article can be found, in the online version, at doi:10.1016/j.neuroimage.2021.118188.

References

Abdi, H., Williams, L.J., 2010. Principal component analysis. WIREs Comput. Stat. 2, 433–459. doi:10.1002/wics.101.

Alexander, W.H., Brown, J.W., 2011. Medial prefrontal cortex as an action-outcome predictor. Nat. Neurosci. 14, 1338–1344. doi:10.1038/nn.2921.

Allen, E.A., Damaraju, E., Plis, S.M., Erhardt, E.B., Eichele, T., Calhoun, V.D., 2014. Tracking whole-brain connectivity dynamics in the resting state. Cereb. Cortex 24, 663–676. doi:10.1093/cercor/bhs352.

Andrews-Hanna, J.R., Reidler, J.S., Sepulcre, J., Poulin, R., Buckner, R.L., 2010. Functional-anatomic fractionation of the brain's default network. Neuron 65, 550–562. doi:10.1016/j.neuron.2010.02.005.

Andrews-Hanna, J.R., Snyder, A.Z., Vincent, J.L., Lustig, C., Head, D., Raichle, M.E., Buckner, R.L., 2007. Disruption of large-scale brain systems in advanced aging. Neuron 56, 924–935. doi:10.1016/j.neuron.2007.10.038.

Baker, A.P., Brookes, M.J., Rezek, I.A., Smith, S.M., Behrens, T., Probert Smith, P.J., Woolrich, M., 2014. Fast transient networks in spontaneous human brain activity. Elife 3, e01867. doi:10.7554/eLife.01867.

Betzel, R.F., Byrge, L., He, Y., Goni, J., Zuo, X.N., Sporns, O., 2014. Changes in structural and functional connectivity among resting-state networks across the human lifespan. Neuroimage 102 (Pt 2), 345–357. doi:10.1016/j.neuroimage.2014.07.067.

Bewick, V., Cheek, L., Ball, J., 2004. Statistics review 10: further nonparametric methods. Crit. Care 8, 196–199. doi:10.1186/cc2857.

Brown, S., Ingham, R.J., Ingham, J.C., Laird, A.R., Fox, P.T., 2005. Stuttered and fluent speech production: an ALE meta-analysis of functional neuroimaging studies. Hum. Brain Mapp. 25, 105–117. doi:10.1002/hbm.20140.

Buckner, R.L., Andrews-Hanna, J.R., Schacter, D.L., 2008. The brain's default network: anatomy, function, and relevance to disease. Ann. N. Y. Acad. Sci. 1124, 1–38. doi:10.1196/annals.1440.011.

Buckner, R.L., Carroll, D.C., 2007. Self-projection and the brain. Trends Cogn. Sci. 11, 49–57. doi:10.1016/j.tics.2006.11.004.

Calhoun, V.D., Miller, R., Pearlson, G., Adali, T., 2014. The chronnectome: time-varying connectivity networks as the next frontier in fMRI data discovery. Neuron 84, 262–274. doi:10.1016/j.neuron.2014.10.015.

Cavanna, F., Vilas, M.G., Palmucci, M., Tagliazucchi, E., 2018. Dynamic functional connectivity and brain metastability during altered states of consciousness. Neuroimage 180, 383–395. doi:10.1016/j.neuroimage.2017.09.065.

Chan, M.Y., Park, D.C., Savalia, N.K., Petersen, S.E., Wig, G.S., 2014. Decreased segregation of brain systems across the healthy adult lifespan. Proc. Natl. Acad. Sci. U. S. A. 111, E4997–E5006. doi:10.1073/pnas.1415122111.

Chen, Y., Wang, W., Zhao, X., Sha, M., Liu, Y., Zhang, X., Ma, J., Ni, H., Ming, D., 2017. Age-related decline in the variation of dynamic functional connectivity: a resting state analysis. Front. Aging Neurosci. 9, 203. doi:10.3389/fnagi.2017.00203.

Corbetta, M., Shulman, G.L., 2002. Control of goal-directed and stimulus-driven attention in the brain. Nat. Rev. Neurosci. 3, 201–215. doi:10.1038/nrn755.

Damaraju, E., Allen, E.A., Belger, A., Ford, J.M., McEwen, S., Mathalon, D.H., Mueller, B.A., Pearlson, G.D., Potkin, S.G., Preda, A., Turner, J.A., Vaidya, J.G., van Erp, T.G., Calhoun, V.D., 2014. Dynamic functional connectivity analysis reveals transient states of dysconnectivity in schizophrenia. Neuroimage Clin. 5, 298–308. doi:10.1016/j.nicl.2014.07.003.

Escrichs, A., Biarnes, C., Garre-Olmo, J., Fernandez-Real, J.M., Ramos, R., Pamplona, R., Brugada, R., Serena, J., Ramio-Torrenta, L., Coll-De-Tuero, G., Gallart, L., Barretina, J., Vilanova, J.C., Mayneris-Perxachs, J., Essig, M., Figley, C.R., Pedraza, S., Puig, J., Deco, G., 2020. Whole-brain dynamics in aging: disruptions in functional connectivity and the role of the rich club. Cereb. Cortex doi:10.1093/cercor/bhaa367.

Faghiri, A., Stephen, J.M., Wang, Y.P., Wilson, T.W., Calhoun, V.D., 2018. Changing brain connectivity dynamics: from early childhood to adulthood. Hum. Brain Mapp. 39, 1108–1117. doi:10.1002/hbm.23896.

Ferreira, L.K., Regina, A.C., Kovacevic, N., Martin Mda, G., Santos, P.P., Carneiro Cde, G., Kerr, D.S., Amaro Jr., E., McIntosh, A.R., Busatto, G.F., 2016. Aging effects on whole-brain functional connectivity in adults free of cognitive and psychiatric disorders. Cereb. Cortex 26, 3851–3865. doi:10.1093/cercor/bhv190.

Fjell, A.M., Sneve, M.H., Grydeland, H., Storsve, A.B., de Lange, A.G., Amlien, I.K., Rogeberg, O.J., Walhovd, K.B., 2015. Functional connectivity change across multiple cortical networks relates to episodic memory changes in aging. Neurobiol. Aging 36, 3255–3268. doi:10.1016/j.neurobiolaging.2015.08.020.

Fransson, P., 2005. Spontaneous low-frequency BOLD signal fluctuations: an fMRI investigation of the resting-state default mode of brain function hypothesis. Hum. Brain Mapp. 26, 15–29. doi:10.1002/hbm.20113.

Friston, K., Frith, C., Liddle, P., Frackowiak, R., 1993. Functional connectivity: the principal-component analysis of large (PET) data sets. J. Cereb. Blood Flow Metab. 13, 5–14.

Friston, K.J., Williams, S., Howard, R., Frackowiak, R.S., Turner, R., 1996. Movement-related effects in fMRI time-series. Magn. Reson. Med. 35, 346–355. doi:10.1002/mrm.1910350312.

Fujita, M., 1982. Adaptive filter model of the cerebellum. Biol. Cybern. 45, 195–206. doi:10.1007/BF00336192.

Fuster, J.M., 2001. The prefrontal cortex–an update: time is of the essence. Neuron 30, 319–333. doi:10.1016/s0896-6273(01)00285-9.

Fuster, J.M., 2004. Upper processing stages of the perception-action cycle. Trends Cogn. Sci. 8, 143–145. doi:10.1016/j.tics.2004.02.004.

Geerligs, L., Saliasi, E., Renken, R.J., Maurits, N.M., Lorist, M.M., 2014. Flexible connectivity in the aging brain revealed by task modulations. Hum. Brain Mapp. 35, 3788–3804. doi:10.1002/hbm.22437.

Golland, Y., Golland, P., Bentin, S., Malach, R., 2008. Data-driven clustering reveals a fundamental subdivision of the human cortex into two global systems. Neuropsychologia 46, 540–553. doi:10.1016/j.neuropsychologia.2007.10.003.

Goulden, N., Khusnulina, A., Davis, N.J., Bracewell, R.M., Bokde, A.L., McNulty, J.P., Mullins, P.G., 2014. The salience network is responsible for switching between the default mode network and the central executive network: replication from DCM. Neuroimage 99, 180–190. doi:10.1016/j.neuroimage.2014.05.052.

Hampton, A.N., O'Doherty, J., 2007. Decoding the neural substrates of reward-related decision making with functional MRI. Proc. Natl. Acad. Sci. U. S. A. 104, 1377–1382. doi:10.1073/pnas.0606297104.

Hindriks, R., Adhikari, M.H., Murayama, Y., Ganzetti, M., Mantini, D., Logothetis, N.K., Deco, G., 2016. Can sliding-window correlations reveal dynamic functional connectivity in resting-state fMRI? Neuroimage 127, 242–256. doi:10.1016/j.neuroimage.2015.11.055.

Hugdahl, K., Raichle, M.E., Mitra, A., Specht, K., 2015. On the existence of a generalized non-specific task-dependent network. Front. Hum. Neurosci. 9, 430. doi:10.3389/fnhum.2015.00430.

Hutchison, R.M., Womelsdorf, T., Allen, E.A., Bandettini, P.A., Calhoun, V.D., Corbetta, M., Della Penna, S., Duyn, J.H., Glover, G.H., Gonzalez-Castillo, J., Handwerker, D.A., Keilholz, S., Kiviniemi, V., Leopold, D.A., de Pasquale, F., Sporns, O., Walter, M., Chang, C., 2013. Dynamic functional connectivity: promise, issues, and interpretations. Neuroimage 80, 360–378. doi:10.1016/j.neuroimage.2013.05.079.

Karahanoglu, F.I., Van De Ville, D., 2015. Transient brain activity disentangles fMRI resting-state dynamics in terms of spatially and temporally overlapping networks. Nat. Commun. 6, 7751. doi:10.1038/ncomms8751.

Kim, J., Criaud, M., Cho, S.S., Diez-Cirarda, M., Mihaescu, A., Coakeley, S., Ghadery, C., Valli, M., Jacobs, M.F., Houle, S., Strafella, A.P., 2017. Abnormal intrinsic brain functional network dynamics in Parkinson's disease. Brain 140, 2955–2967. doi:10.1093/brain/awx233.

Koelsch, S., Fritz, T., DY, V.C., Muller, K., Friederici, A.D., 2006. Investigating emotion with music: an fMRI study. Hum. Brain Mapp. 27, 239–250. doi:10.1002/hbm.20180.

Kopell, N.J., Gritton, H.J., Whittington, M.A., Kramer, M.A., 2014. Beyond the connectome: the dynome. Neuron 83, 1319–1328. doi:10.1016/j.neuron.2014.08.016.

la Iglesia-Vaya, M.d., Molina-Mateo, J., Jose, M., S, A., Marti-Bonmati, L., 2013. Brain connections – resting state fMRI functional connectivity. In: Fountas, K.N. (Ed.), Novel Frontiers of Advanced Neuroimaging (Ed.). IntechOpen doi:10.5772/52273.

Le Martelot, E., Hankin, C., 2013. Fast multi-scale detection of relevant communities in large-scale networks. Comput. J. 56, 1136–1150. doi:10.1093/comjnl/bxt002.

Liu, W., Kohn, N., Fernández, G., 2020. The dynamic transition between neural states is associated with the flexible use of memory. bioRxiv doi:10.1101/2020.07.04.188235.

Liu, Z., Rolls, E.T., Liu, Z., Zhang, K., Yang, M., Du, J., Gong, W., Cheng, W., Dai, F., Wang, H., Ugurbil, K., Zhang, J., Feng, J., 2019. Brain annotation toolbox: exploring the functional and genetic associations of neuroimaging results. Bioinformatics 35, 3771–3778. doi:10.1093/bioinformatics/btz128.

Malagurski, B., Liem, F., Oschwald, J., Mérillat, S., Jäncke, L., 2020. Longitudinal functional brain network reconfiguration in healthy aging. Hum. Brain Mapp. 41, 4829–4845. doi:10.1002/hbm.25161.

Menon, V., 2011. Large-scale brain networks and psychopathology: a unifying triple network model. Trends Cogn. Sci. 15, 483–506. doi:10.1016/j.tics.2011.08.003.

Monteiro, T.S., King, B.R., Zivari Adab, H., Mantini, D., Swinnen, S.P., 2019. Age-related differences in network flexibility and segregation at rest and during motor performance. Neuroimage 194, 93–104. doi:10.1016/j.neuroimage.2019.03.015.

Morcom, A.M., Fletcher, P.C., 2007. Does the brain have a baseline? Why we should be resisting a rest. Neuroimage 37, 1073–1082. doi:10.1016/j.neuroimage.2006.09.013.

Naik, S., Banerjee, A., Bapi, R.S., Deco, G., Roy, D., 2017. Metastability in Senescence. Trends Cogn. Sci. 21, 509–521. doi:10.1016/j.tics.2017.04.007.

Nakamichi, N., Takamoto, K., Nishimaru, H., Fujiwara, K., Takamura, Y., Matsumoto, J., Noguchi, M., Nishijo, H., 2018. Cerebral hemodynamics in speech-related cortical areas: articulation learning involves the inferior frontal gyrus, ventral sensory-motor cortex, and parietal-temporal Sylvian area. Front Neurol 9, 939. doi:10.3389/fneur.2018.00939.

O'Regan, J.K., Noe, A., 2001. A sensorimotor account of vision and visual consciousness. Behav. Brain Sci. 24, 939–973. doi:10.1017/s0140525x01000115, discussion 973-1031.

Pinotsis, D.A., Hansen, E., Friston, K.J., Jirsa, V.K., 2013. Anatomical connectivity and the resting state activity of large cortical networks. Neuroimage 65, 127–138. doi:10.1016/j.neuroimage.2012.10.016.

Porrill, J., Dean, P., Anderson, S.R., 2013. Adaptive filters and internal models: multilevel description of cerebellar function. Neural Netw. 47, 134–149. doi:10.1016/j.neunet.2012.12.005.

Preti, M.G., Bolton, T.A., Van De Ville, D., 2017. The dynamic functional connectome: state-of-the-art and perspectives. Neuroimage 160, 41–54. doi:10.1016/j.neuroimage.2016.12.061.

Ramnani, N., Behrens, T.E., Johansen-Berg, H., Richter, M.C., Pinsk, M.A., Andersson, J.L., Rudebeck, P., Ciccarelli, O., Richter, W., Thompson, A.J., Gross, C.G., Robson, M.D., Kastner, S., Matthews, P.M., 2006. The evolution of prefrontal inputs to the cortico-pontine system: diffusion imaging evidence from Macaque monkeys and humans. Cereb. Cortex 16, 811–818. doi:10.1093/cercor/bhj024.

Reinen, J.M., Chen, O.Y., Hutchison, R.M., Yeo, B.T.T., Anderson, K.M., Sabuncu, M.R., Ongur, D., Roffman, J.L., Smoller, J.W., Baker, J.T., Holmes, A.J., 2018. The human cortex possesses a reconfigurable dynamic network architecture that is disrupted in psychosis. Nat. Commun. 9, 1157. doi:10.1038/s41467-018-03462-y.

Rolls, E.T., Joliot, M., Tzourio-Mazoyer, N., 2015. Implementation of a new parcellation of the orbitofrontal cortex in the automated anatomical labeling atlas. Neuroimage 122, 1–5. doi:10.1016/j.neuroimage.2015.07.075.

Sala-Llonch, R., Bartres-Faz, D., Junque, C., 2015. Reorganization of brain networks in aging: a review of functional connectivity studies. Front Psychol 6, 663. doi:10.3389/fpsyg.2015.00663.

Salami, A., Pudas, S., Nyberg, L., 2014. Elevated hippocampal resting-state connectivity underlies deficient neurocognitive function in aging. Proc. Natl. Acad. Sci. U. S. A. 111, 17654–17659. doi:10.1073/pnas.1410233111.

Schaefer, A., Margulies, D.S., Lohmann, G., Gorgolewski, K.J., Smallwood, J., Kiebel, S.J., Villringer, A., 2014. Dynamic network participation of functional connectivity hubs assessed by resting-state fMRI. Front. Hum. Neurosci. 8, 195. doi:10.3389/fnhum.2014.00195.

Shannon, C.E., 1951. Prediction and Entropy of Printed English. Bell Syst. Tech. J. 30, 50–64. doi:10.1002/j.1538-7305.1951.tb01366.x.

Shine, J.M., Bissett, P.G., Bell, P.T., Koyejo, O., Balsters, J.H., Gorgolewski, K.J., Moodie, C.A., Poldrack, R.A., 2016. The dynamics of functional brain networks: integrated network states during cognitive task performance. Neuron 92, 544–554. doi:10.1016/j.neuron.2016.09.018.

Smith, S.M., Nichols, T.E., Vidaurre, D., Winkler, A.M., Behrens, T.E., Glasser, M.F., Ugurbil, K., Barch, D.M., Van Essen, D.C., Miller, K.L., 2015. A positive-negative mode of population covariation links brain connectivity, demographics and behavior. Nat. Neurosci. 18, 1565–1567. doi:10.1038/nn.4125.

Spreng, R.N., 2012. The fallacy of a "task-negative" network. Front. Psychol. 3, 145. doi:10.3389/fpsyg.2012.00145.

Sridharan, D., Levitin, D.J., Menon, V., 2008. A critical role for the right fronto-insular cortex in switching between central-executive and default-mode networks. Proc. Natl. Acad. Sci. U. S. A. 105, 12569–12574. doi:10.1073/pnas.0800005105.

Staffaroni, A.M., Brown, J.A., Casaletto, K.B., Elahi, F.M., Deng, J., Neuhaus, J., Cobigo, Y., Mumford, P.S., Walters, S., Saloner, R., Karydas, A., Coppola, G., Rosen, H.J., Miller, B.L., Seeley, W.W., Kramer, J.H., 2018. The longitudinal trajectory of default mode network connectivity in healthy older adults varies as a function of age and is associated with changes in episodic memory and processing speed. J. Neurosci. 38, 2809–2817. doi:10.1523/JNEUROSCI.3067-17.2018.

Thompson, G.J., 2018. Neural and metabolic basis of dynamic resting state fMRI. Neuroimage 180, 448–462. doi:10.1016/j.neuroimage.2017.09.010.

Tian, L., Li, Q., Wang, C., Yu, J., 2018. Changes in dynamic functional connections with aging. Neuroimage 172, 31–39. doi:10.1016/j.neuroimage.2018.01.040.

Tomasi, D., Volkow, N.D., 2012. Aging and functional brain networks. Mol. Psychiatry 17, 549–558. doi:10.1038/mp.2011.81.

Tomasino, B., Canderan, C., Marin, D., Maieron, M., Gremese, M., D'Agostini, S., Fabbro, F., Skrap, M., 2015. Identifying environmental sounds: a multimodal mapping study. Front. Hum. Neurosci. 9, 567. doi:10.3389/fnhum.2015.00567.

Vidaurre, D., Smith, S.M., Woolrich, M.W., 2017. Brain network dynamics are hierarchically organized in time. Proc. Natl. Acad. Sci. U. S. A. 114, 12827–12832. doi:10.1073/pnas.1705120114.

Viviano, R.P., Raz, N., Yuan, P., Damoiseaux, J.S., 2017. Associations between dynamic functional connectivity and age, metabolic risk, and cognitive performance. Neurobiol. Aging 59, 135–143. doi:10.1016/j.neurobiolaging.2017.08.003.

Wolpert, D.M., Miall, R.C., Kawato, M., 1998. Internal models in the cerebellum. Trends Cogn. Sci. 2, 338–347. doi:10.1016/s1364-6613(98)01221-2.

Yao, Y., Lu, W.L., Xu, B., Li, C.B., Lin, C.P., Waxman, D., Feng, J.F., 2013. The increase of the functional entropy of the human brain with age. Sci. Rep. 3, 2853. doi:10.1038/srep02853.

Yeo, B.T.T., Krienen, F.M., Sepulcre, J., Sabuncu, M.R., Lashkari, D., Hollinshead, M., Roffman, J.L., Smoller, J.W., Zoller, L., Polimeni, J.R., Fischl, B., Liu, H.S., Buckner, R.L., 2011. The organization of the human cerebral cortex estimated by intrinsic functional connectivity. J. Neurophysiol. 106, 1125–1165. doi:10.1152/jn.00338.2011.

Zabelina, D.L., Andrews-Hanna, J.R., 2016. Dynamic network interactions supporting internally-oriented cognition. Curr. Opin. Neurobiol. 40, 86–93. doi:10.1016/j.conb.2016.06.014.

Zhang, J., Cheng, W., Liu, Z., Zhang, K., Lei, X., Yao, Y., Becker, B., Liu, Y., Kendrick, K.M., Lu, G., Feng, J., 2016. Neural, electrophysiological and anatomical basis of brain-network variability and its characteristic changes in mental disorders. Brain 139, 2307–2321. doi:10.1093/brain/aww143.

Zhou, Q.J., Zhang, L., Feng, J.F., Lo, C.Y.Z., 2019. Tracking the main states of dynamic functional connectivity in resting state. Front. Neurosci. 13. doi:10.3389/fnins.2019.00685.

Zonneveld, H.I., Pruim, R.H.R., Bos, D., Vrooman, H.A., Muetzel, R.L., Hofman, A., Rombouts, S.A.R.B., van der Lugt, A., Niessen, W.J., Ikram, M.A., Vernooij, M.W., 2019. Patterns of functional connectivity in an aging population: the Rotterdam study. Neuroimage 189, 432–444. doi:10.1016/j.neuroimage.2019.01.041.